

Article

Use of Processed Sugarcane Bagasse Ash in Concrete as Partial Replacement of Cement: Mechanical and Durability Properties

Shazim Ali Memon ^{1,*}, Usman Javed ², Muhammad Izhar Shah ³ and Asad Hanif ^{4,5}

¹ Department of Civil and Environmental Engineering, School of Engineering and Digital Sciences, Nazarbayev University, Astana 010000, Kazakhstan

² School of Civil and Mechanical Engineering, Curtin University, Perth, WA 6102, Australia

³ Department of Civil Engineering, COMSATS Institute of Information and Technology, Abbottabad 22060, Pakistan

⁴ Civil and Environmental Engineering Department, King Fahd University of Petroleum and Minerals (KFUPM), Dhahran 31261, Saudi Arabia

⁵ Interdisciplinary Research Center for Construction and Building Materials, KFUPM, Dhahran 31261, Saudi Arabia

* Correspondence: shazim.memon@nu.edu.kz

Abstract: Using biomass waste as supplementary cementing material (SCM) in concrete has attracted researchers' attention for efficient waste utilization and reducing cement demand. Sugarcane bagasse ash (SCBA) is one such example of biomass waste. It is an agricultural waste obtained when sugarcane bagasse from the sugar industry is used for power generation and disposed of in open-air dumping sites. Its waste disposal causes the generation of particulate matter, degrading air quality. In this study, the effect of processed SCBA as SCM in concrete has been investigated. The processing of the SCBA involved the removal of fibrous and carbon-containing particles by sieving followed by grinding. The SCBA was ground for 45 min until the surface area was comparable to that of cement and was then used for further characterization and incorporation into concrete. The 45 min grinding time resulted in 2.92 times higher pozzolanic reactivity of the SCBA. The SCBA was incorporated by replacing cement in different weight fractions (10%, 20%, 30%, 40%) in concrete. Test results showed that the concrete workability increased with SCBA incorporation, whereas the resulting concrete density was reduced. The results of the mechanical properties, including compressive strength and hardened density, were enhanced upon the cement replacement by SCBA. Concrete containing 30% SCBA can be used for structural applications as its 28 days compressive strength was 21 MPa, which complies with ACI 318-16 specifications. Concrete resistance against scaling and leaching due to adverse effects of sulfuric and hydrochloric acid considerably increased with SCBA addition and was due to microstructure densification by secondary hydrates formation as lower portlandite content was detected by thermogravimetric analysis. Hence, SCBA processing increases its reactivity, as reflected by the improved mechanical properties and greater durability of SCBA-incorporated concrete.

Keywords: sugarcane bagasse ash; waste disposal; structural concrete; pozzolanic activity; durability



Citation: Memon, S.A.; Javed, U.; Shah, M.I.; Hanif, A. Use of Processed Sugarcane Bagasse Ash in Concrete as Partial Replacement of Cement: Mechanical and Durability Properties. *Buildings* **2022**, *12*, 1769. <https://doi.org/10.3390/buildings12101769>

Academic Editor: Ahmed Senouci

Received: 3 October 2022

Accepted: 19 October 2022

Published: 21 October 2022

Publisher's Note: MDPI stays neutral with regard to jurisdictional claims in published maps and institutional affiliations.



Copyright: © 2022 by the authors. Licensee MDPI, Basel, Switzerland. This article is an open access article distributed under the terms and conditions of the Creative Commons Attribution (CC BY) license (<https://creativecommons.org/licenses/by/4.0/>).

1. Introduction

Concrete is the most widely used manmade material on earth [1]. Its use has exponentially increased with the rapid increase in the world population. Five percent of emissions of the total greenhouse gases emerge from the concrete industry, which are responsible for global climate change [2]. According to statistics, more than 4 billion tons of carbon emission is linked to the annual production of cement which is over 4 billion tons [3,4]. Moreover, cement production has increased the concentration of carbon footprints up to 380 ppm in the atmosphere, which is expected to rise up to 800 ppm by 2100 [5]. Nowadays, different supplementary cementing materials (SCMs), such as metakaolin, fly ash, slag, and

silica fume are used in the construction industry to limit the use of cement and consequently to reduce carbon emissions [6,7].

Sugarcane is among the most abundantly growing crops in the world [8,9]. The annual sugarcane production in the subcontinent is 0.3 billion tons, contributing 1/5th of its worldwide production. Ten million tons of sugarcane bagasse ash (SCBA) are annually produced by burning sugarcane bagasse for power production [10]. The SCBA thus produced is difficult to dispose of due to the eco-hazardous nature of SCBA and the shortage of dumping sites in the recent population boom [11]. The inappropriate disposal of SCBA causes environmental degradation due to the dispersal of particulate matter and other air pollutants in the atmosphere. These air pollutants cause several respiratory diseases when inhaled into the human body [12,13]. The World Health Organization (WHO) reported that elevated air pollution caused 6.7% of deaths worldwide in 2012 [14].

SCBA is one of the SCMs used in concrete, which is known to improve concrete properties when used as SCM. However, very few researchers have investigated its optimization by calcination and reduction in its particle size [15,16]. The crystallographic phase transformation of SCBA was the subject of a study by Sultana and Rahman [15], in which they investigated the effect of calcination temperature on crystallographic properties. Test results indicated that SCBA changed from the amorphous to the crystalline state between 800 °C to 1000 °C. Cordeiro et al. [17] revealed that the optimum calcination temperature of SCBA for minimum carbon content and maximum surface area was 600 °C maintained for 3 h. Rukzon and Chindapasirt [18] produced durable concrete using bagasse ash in high-strength concrete. A 30% incorporation of SCBA in concrete showed better durability in terms of greater chloride ion penetration resistance due to secondary hydrates. Sabestin et al. [19] utilized SCBA in reactive powder concrete and concluded that the maximum increase in compressive strength was observed at 17.5% cement replacement. Xu et al. [20] investigated the effects of SCBA incorporation on resulting concrete properties and showed improved physical, mechanical, and durability attributes of modified concretes. Bahurudeen and Santhanam optimized the processing of SCBA by grinding and sieving the fibrous particles for optimizing the pozzolanic potential of SCBA in concrete; however, a detailed investigation of SCBA on the mechanical and durability attributes of the resulting concrete is yet to be conducted.

This research article provides a detailed investigation of the effect of processing SCBA on the fresh physico-mechanical properties and the durability resistance of concrete. SCBA processing included grinding for one hour in a ball mill followed by sieving through a 75 µm sieve to remove coarser particles containing higher carbon content and to achieve better pozzolanic reactivity. SCBA pozzolanic activity was determined by the Chapelle test, whereas SCBA was incorporated afterwards by replacing 10%, 20%, 30%, and 40% of cement in concrete and testing for fresh concrete tests. The fresh and hardened-state properties of the SCBA-incorporated concrete were evaluated. Additionally, thermogravimetric analysis (TGA) was conducted on the SCBA-incorporated concrete to qualitatively determine the extent of pozzolanic activity. The successful incorporation of SCBA in concrete offers an environmentally friendly alternative to its disposal. It would limit cement use in concrete without adversely affecting the resulting properties.

2. Materials and Experimental Methods

2.1. Raw Materials

Ordinary Portland cement (OPC) under the 'Bestway' brand name, complying with ASTM C150 and having a fineness value of 2671 cm²/g was used in this study. Lawrencepur river sand (fineness modulus 2.93) complying with ASTM C33 was used as fine aggregate. Coarse aggregate from Dorr River quarry, Havelian-KPK, Pakistan, was used. The physical properties of the raw materials are given in Table 1.

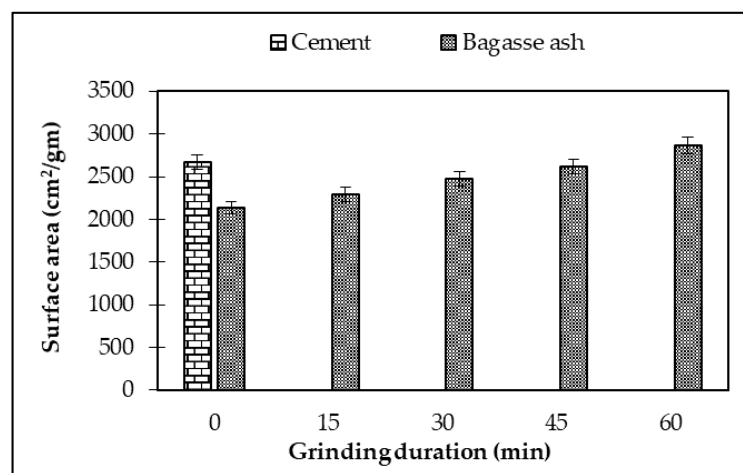
Table 1. Raw materials characteristics.

Description	Fine Aggregate	Bagasse Ash (SCBA)	Coarse Aggregate
Water absorption (%)	1.9	-	0.2
Specific Gravity	2.6	1.35	2.64

In Pakistan, SCBA is usually obtained by burning sugarcane bagasse as a fuel in the sugar industry for powering boilers, thus producing waste bagasse ash. Therefore, the SCBA used in this research was obtained from the sugar industry in Sakhakot-Malakand division, Pakistan, for use as SCM in concrete.

2.2. Material Processing

Removing the fibrous and unburnt carbon particles from raw bagasse ash is imperative, as it reduces its reactivity in the cementitious matrix. According to Bahurudeen and Santhanam, removing such particles by sieving and grinding to achieve a fineness similar to that of cement significantly increases its reactivity in the cementitious matrix [21]. Hence, to increase the SCBA pozzolanic activity, it was sieved through sieve #200 (75 μm) and then milled in a ball mill. The weight ratio of grinding media to SCBA value was kept at 5 and operated at 66 revolution per minutes (rpm) for different grinding durations of 15, 30, 45, and 60 min to achieve a surface area comparable to that of cement. After grinding SCBA for the specified durations, the surface area of the resulting ash was determined in a Blaine air-permeability apparatus as per ASTM standard C204 [22]. The results of the specific surface areas after grinding SCBA for various durations are shown in Figure 1, which clearly depicts that the specific surface area increased with the increasing duration of grinding. The maximum value of 2862 cm^2/g was observed for the grinding duration of 60 min, whereas the specific surface area of SCBA at the grinding duration of 45 min was 2617.8 cm^2/g and was closer to that of cement. Hence, SCBA ground for a duration of 45 min was used for further investigation as a supplementary cementitious material in concrete.

**Figure 1.** Comparison of SCBA surface area with cement for different grinding durations.

2.3. Chemical Reactivity and Microstructural Characterization of SCBA

Table 2 shows the chemical composition of ground SCBA determined by X-ray fluorescence (XRF). The cumulative sum of silica, alumina, and iron in SCBA was found to be 77.47%, which meets the ASTM C618 requirement of pozzolanic materials [23]. The presence of phosphorous pentoxide (P_2O_5) was found at 1.98%, which might have originated from the use of fertilizers. Morales et al. [24] reported the presence of 2.09 and 2.15% of P_2O_5 at calcination temperatures of 800 $^\circ\text{C}$ and 1000 $^\circ\text{C}$, respectively. Similarly, Sultana and Rahman [25] found the presence of P_2O_5 at 3.37%, 3.42%, 3.40%, and 3.46% at calcination

temperatures of 400 °C, 600 °C, 800 °C, and 1000 °C, respectively. The oxide composition of the SCBA sample is shown in Table 2 after the removal of fibrous carbon-rich particles by sieving through a 75 µm sieve.

Table 2. Chemical (oxide) composition of sugarcane bagasse ash (SCBA) and OPC.

Description	SCBA	OPC
SiO ₂	66.7	21.29
Al ₂ O ₃	9.24	4.82
Fe ₂ O ₃	1.53	3.88
CaO	10.07	65.12
MgO	4.6	2.21
P ₂ O ₅	1.98	-
K ₂ O	2.44	0.45
Na ₂ O	1.3	-
TiO ₂	0.22	-
MnO	0.02	-
LOI	1.9	2.23
Moisture content	1.1	-

The crystallographic phases in SCBA were identified using X-ray diffraction (XRD) in MATCH software aided by the International Crystallographic Diffraction Database (ICDD). The XRD results presented in Figure 2 indicate the presence of quartz and cristobalite (PDF No. 46-1045, 39-1425) at diffraction angle (2θ) values of 5.85 (d = 15.09), 20.85 (d = 4.25), 26.65 (d = 3.34), 29.35 (d = 3.04), 68.20 (d = 1.37), and 50.05 (d = 1.82), respectively. The presence of a higher concentration of silica in the form of quartz was identified in the XRD pattern marked by intense peaks. However, the intensity of the peak is proportionate with that of a mineral component producing it [26].

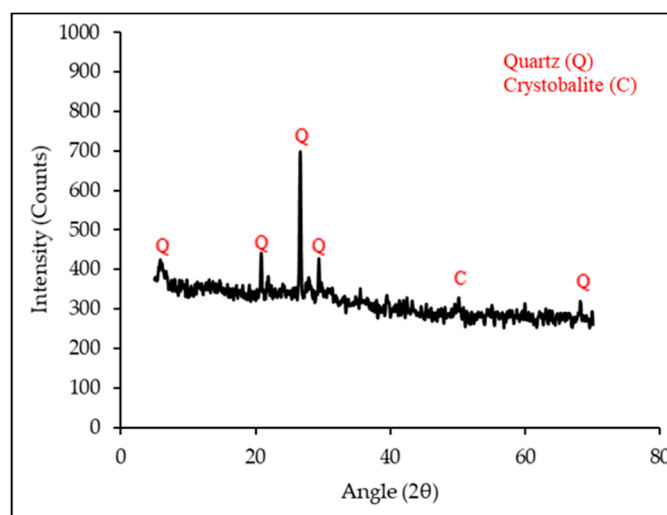


Figure 2. XRD pattern of processed SCBA (sieved and ground for 45 min).

The pozzolanic potential of ground SCBA was ascertained by the Chapelle activity test as per French norm NF P 18-513 [27]. Free portlandite (Ca(OH)₂) was determined in a 250 mL solution containing 2 g cement and 1 g ash, which was subsequently heated at 90 °C for 16 h in a drying oven. The unreacted Ca(OH)₂ amount in the solution was found by acid-base titration that yielded the equivalent volume of hydrochloric acid required to neutralize the free Ca(OH)₂ in control as well as the ash-blended sample. Fixed Ca(OH)₂ was calculated by using Equation (1).

$$\text{mg of Ca(OH)}_2 \text{ fixed/g} = 2 \times ((V_1 - V_2)) / V_1 \times 74/56 \times 1000 \quad (1)$$

V_1 = volume of 0.1N HCL (ml) consumed to titrate 25 mL of solution from the control sample.

V_2 = volume of 0.1N HCL (ml) consumed to titrate 25 mL of solution from the blended sample.

The results of the Chapelle activity test presented in Table 3 show that the Chapelle activity of the SCBA was 1293.9 CaO(mg/g), and the pozzolanic potential of the SCBA was 2.92 times higher than that of the standard sample (330 CaO mg/g). A higher Chapelle activity value is indicative of the improved pozzolanic potential of the SCBA due to a reduced concentration of friable particles that may hinder its reactivity [28,29].

Table 3. Chapelle test results.

Titration Volume of HCL for Control Mixture (V1) *	Titration Volume of HCL for Ash Mixture (V2) *	Chapelle Activity = CaO(mg/g) = ((V1 – V2)/V1) * 2642.86	% Increase w.r.t Standard (330 mg/g)
19.2	9.8	1293.9	+ 292

* Chapelle activity results are average of three trials.

The microstructure of the ground SCBA sample was studied by scanning electron microscopy (SEM) imaging using model JSM-5910 JEOL, Japan. The micrographs of the SCBA are presented in Figure 3. In general, SCBA has a heterogeneous nature as it contains a variety of particle shapes, including prismatic, elongated, rounded, needle, flat, oval, and irregular shapes. The particle shapes also vary in size range. Needle and oval-shaped particles were up to 50 μm in size, while irregular-shaped particles were around 20 μm and, according to the literature, are mainly rich in reactive silica [21,30]. Perforations with a size of a few hundred nanometers on the surface of SCBA particles induce its adsorptive nature, thus increasing the water retaining capacity of the ash.

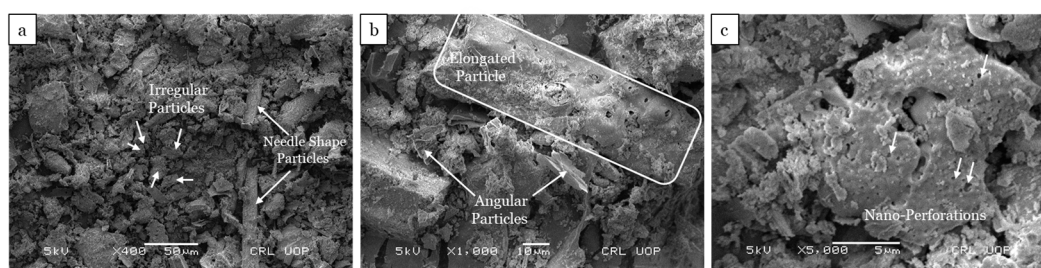


Figure 3. SEM micrographs of ground SCBA. (a) Irregular Particles and Needle Shape Particles; (b) Elongated Particle and Angular Particles; (c) Nano-Perforations.

2.4. Mixture Proportioning and Specimens Preparation

The target design strength of the concrete was set as 21 MPa with a cement content of 366 kg/m^3 . The mix proportions are shown in Table 4. In the concrete mixes, cement was replaced with SCBA by 0%, 10%, 20%, 30%, and 40% by weight of cement and are represented by CM, 10BC, 20BC, 30BC, and 40BC, respectively. A fixed water-to-binder ratio of 0.5 was adopted for a fair comparison.

Table 4. Concrete mix proportions (Kg/m^3).

Mix Designation	Cement	Bagasse Ash	W/C	Fine Aggregate	Coarse Aggregate	Water
0BC(CM)	366	0	0.5	742.3	1013.5	183
10BC	329.4	36.6	0.5	742.3	1013.5	183
20BC	292.8	73.2	0.5	742.3	1013.5	183
30BC	256.2	109.8	0.5	742.3	1013.5	183
40BC	219.6	146.4	0.5	742.3	1013.5	183

2.5. Casting and Curing of Specimens

The 150 mm × 150 mm × 150 mm concrete cube specimens were fabricated at room temperature, as per ASTM standard C 511 [31]. After demolding, the specimens were mist cured at 24 ± 1 °C for subsequent testing for mechanical and durability properties at a specified age.

2.6. Testing Program

The effect of SCBA incorporation in concrete as SCM was evaluated by investigating various fresh and hardened concrete properties. Fresh concrete properties including slump, fresh state density, and compaction factor tests were performed confirming ASTM C 143 [32], ASTM C138M-01 [33], and BS 1881-103:1993 [34], respectively. Hardened concrete properties, including compressive strength, hardened density, water absorption, sorptivity, UPV, and acid attack tests were performed to investigate the physico-mechanical properties and durability aspects of the SCBA-incorporated concrete. The compressive strength of the concrete specimens was determined as per BS 1881: Part 116: 1983, hardened density and water absorption were determined complying with ASTM C642 [35], and ultrasonic pulse velocity was determined with ASTM C597 [36], respectively. Sorptivity in terms of capillary suction of water through the cross-section of the SCBA-incorporated concrete intact with water was determined by dipping a 2 mm depth of the oven-dried concrete cubes into water [37]. The water tends to rise through capillary suction, thus increasing the weight of the concrete sample. The specimens were weighed at various time intervals. Sorptivity was determined by plotting the volume of water absorbed per unit cross-sectional area against the square root of time and is expressed in $\text{mm}/\text{min}^{0.5}$.

In order to determine the durability of the SCBA-incorporated concrete, the samples were immersed in a 5% concentrated sulfuric and hydrochloric acid solution separately for 28 days after completing 28 days of curing. Later, the weight loss and strength loss were recorded after oven drying the samples for 24 h to assess their degree of deterioration. In order to determine the pozzolanic activity of concrete, thermogravimetric analysis (TGA) was conducted on cement mortar extracted from the control and 10BC concrete specimens at a curing age of 90 days. The extracted cement paste chunks (10 mm × 10 mm) of the mentioned mixes were placed in acetone for 24 h to stop hydration [38]. Then, the cement mortar chunks were oven dried at 100 ± 5 °C for 4 h followed by grinding. The decrease in weight of the specimen was recorded up to 900 °C with an incremental temperature of 10 °C/min.

3. Discussions of Results

3.1. Fresh-State Properties of Concrete

The results of the fresh concrete properties are shown in Figures 4–6. The slump values for the CM, 10BC, 20BC, 30BC, and 40BC mixes were found as 29, 30, 47.5, 52.5, and 58 mm, respectively. A 3.4–10.47% increase in slump was observed with the SCBA addition. The maximum value of slump was observed for the 40BC mix, whereas the minimum value was recorded for the CM mix. The water demand of the concrete increased with the incorporation of SCBA, owing to the presence of carbon content in it. Similar behavior of increased water demand was observed upon the addition of SCBA as SCM in concrete [39]. Increased workability as depicted by higher slump values was attained, which is attributed to the increased water demand with the SCBA addition [40].

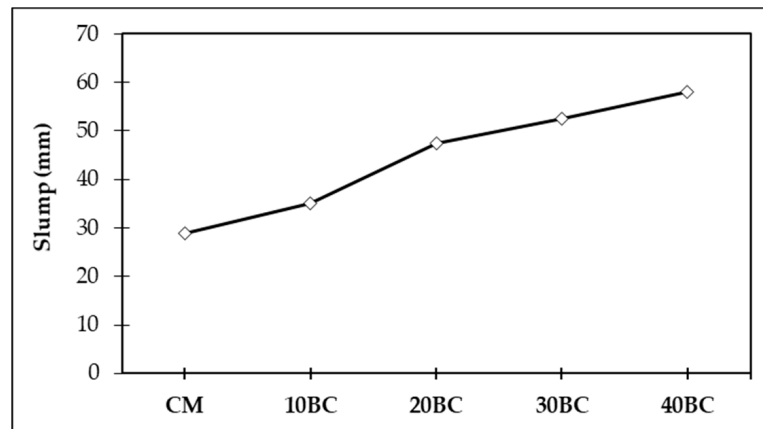


Figure 4. Comparison of slump values among several concrete mixes.

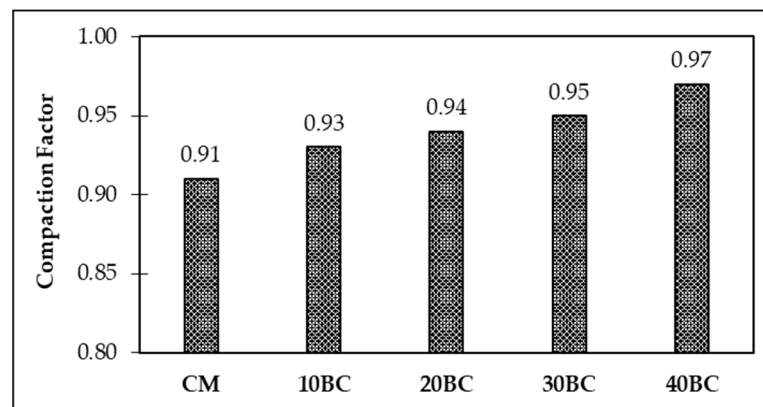


Figure 5. Compaction factor values of different concrete mixes.

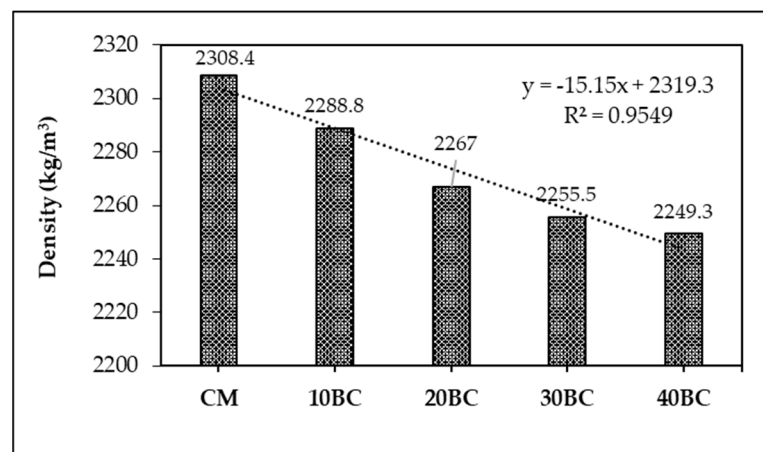


Figure 6. Fresh concrete density of concrete mixes.

Compaction factor is another measure for fresh concrete workability that can be estimated as the ratio of partially compacted specimen weight to completely compacted specimen weight. The results of the compaction factor revealed that the workability of the SCBA-additive concrete increased with SCBA content, depicting that it can flow more easily. The percentage increase in the compaction factor compared to that of the control concrete at the highest replacement level (40BC) was 6.59. The reason for the increase in workability with SCBA content in concrete has been discussed earlier.

The maximum fresh density (Figure 6) was found for the control mix (CM) as 2308.4 kg/m³. The fresh density decreased with increasing SCBA weight fraction. The decrease in fresh concrete density for the SCBA-incorporated concretes was found as 0.85–2.62% compared to CM, which is attributed to the lower specific gravity of SCBA than of cement. Various published studies also reported similar trends of fresh density. Zareei et al. [41] and Le et al. [42] reported the reduction in the fresh density of concrete with increasing SCBA content, which was attributed to its lower specific weight than cement.

3.2. Water Absorption

Water absorption is the concrete permeability indicator since it represents the amount of water penetrating from the surfaces of concrete, imitating the exposure of a marine environment or saturated soil to the concrete. Higher permeability, typically, is associated with higher exposure to drying and wetting cycles and may cause the leaching of portlandite upon several cycles of exposure to water, thus inducing the porosity in concrete.

Figure 7 shows the water absorption of hardened concretes. The results depict the decreasing trend of water absorption with increasing ash content and curing age. The reduction in water absorption at 7 days was observed comparative to the control concrete for 10BC, 20BC, 30BC, and 40BC as 11.42, 22.1, 33.8, and 46.9%, whereas the reduction in water absorption of the concrete mixes at 90 days for 10BC, 20BC, 30BC, and 40BC was 7.9, 17.2, 26.5, and 33.1%. The reduction in water absorption in the control concrete compared to the 40BC mix is higher at 7 days than 90 days of curing which might be due to a higher rate of hydration in the control concrete. However, at higher curing ages, the densification of the concrete microstructure by filling capillary voids [43] due to the pozzolanic potential of SCBA improves concrete performance against capillary suction and water ingress [1,44]. The reduction in water absorption at higher curing ages is due to the replacement of portlandite (having a lower density) with secondary calcium silicate hydrate (C–S–H) gel (having a higher density) due to the pozzolanic reactivity of SCBA.

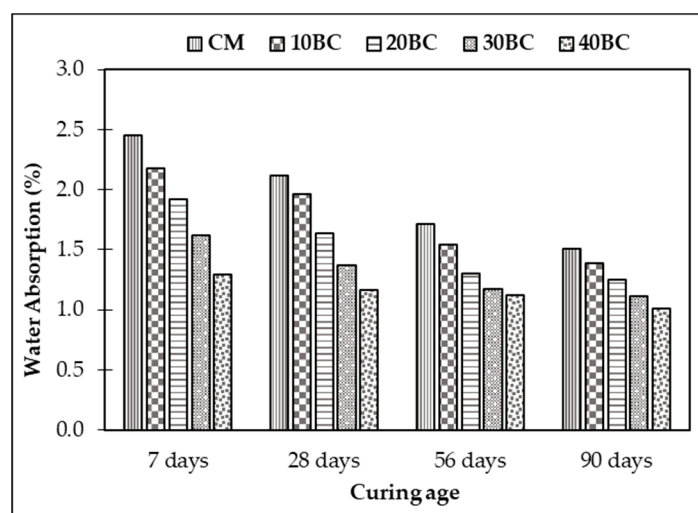


Figure 7. Water absorption (%).

The trend in water absorption for all concrete mixes containing SCBA was determined by polynomial regression equations at varying curing ages, as shown in Figure 8. The trend lines having a negative slope indicate decreasing water absorption with the increasing SCBA amount. The correlation coefficients at all ages were found to be ≥ 0.98 , signifying high data reliability. Hence, it is deduced that SCBA incorporation in concrete causes a decrease in water absorption.

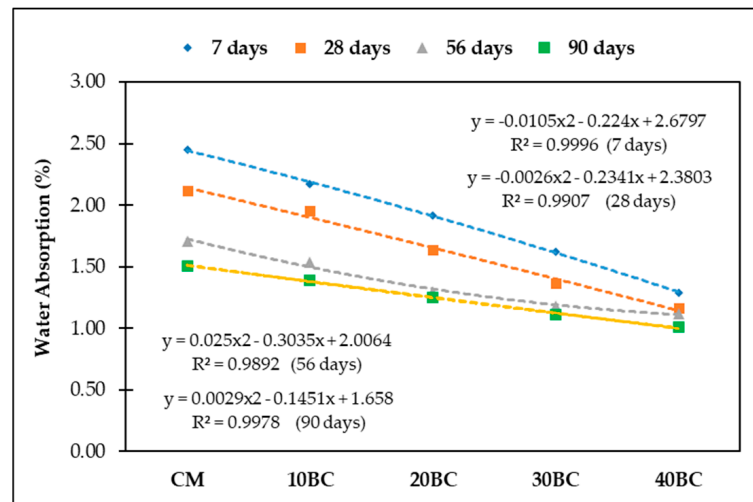


Figure 8. Regression equations for water absorption for different concrete mixes.

3.3. Compressive Strength

The results of the compressive strength of the SCBA-incorporated concrete are shown in Figure 9. It is seen that the strength increases with age. Although the 7-day strength of the SCBA-modified concretes was found to be lower than the control mix, after 28 days, the concretes with 10% SCBA showed increased strength. Compressive strength (in MPa) of the CM and the 10BC at 7, 28, 56, and 90 days of curing was found as 19.40, 23.14, 24.97, 27.21 and 14.96, 23.94, 25.77, 29.64, respectively. The compressive strength of the 10BC mix was higher than that of the CM mix by 3.34%, 3.10%, and 8.2% at 28, 56, and 90 days, respectively. The disparity among the results obtained from different specimens was small (less than 5%). Although the compressive strength increased with curing age, the strength development of concrete mixes incorporating SCBA showed lower concrete strength than the control concrete at 7 days, which is attributed to the dilution effect of cement in the concrete mixes and low pozzolanic activity at early ages [21].

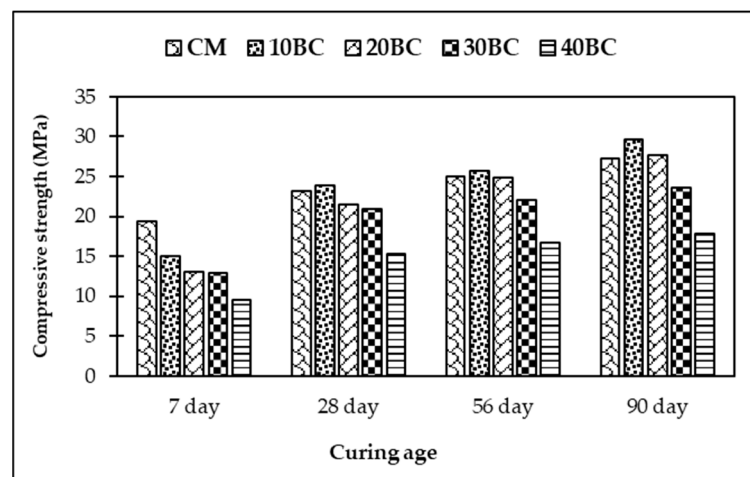


Figure 9. Compressive strengths at different ages.

The 28-d compressive strength of the 30BC was determined as 21 MPa, which qualifies it for use in structural applications conforming to ACI 318, whereas it remained 9.24% lower than that of the control concrete. Moreover, the compressive strength of the 10BC mix was tested as 23.94 MPa which was 3.29% higher than that of the control concrete. On 28 days and onward, the compressive strength of the 10BC mix remained higher than the control concrete at all curing ages indicating optimal strength development. The

compressive strength dropped upon further replacement of SCBA due to the dilution effect of cement in the mix. Other than the optimum mix (10BC), the strength development of the SCBA-added concrete for the 20BC, 30BC, and 40BC at 28 days was 92.62%, 90.76%, and 66.12%; at 56 days it was 99.84%, 88.11%, and 66.69%; and at 90 days it was 101.50%, 86.77%, and 65.79%, respectively. The highest values of strength development compared to the control concrete for the 20BC, 30BC, and 40BC mixes were 101.50%, 90.76%, and 65.79%, respectively.

The increased compressive strength of the 10% SCBA-incorporated concrete at 28 days was prominent owing to secondary hydrates formation with reduced portlandite content due to reactive SCBA particles [41,45,46]. In the concrete mixes with SCBA > 10%, the amount of bagasse ash was higher than the amount needed for the reaction with portlandite; thus, the excess of unreacted silica disturbed the balance between the silica to alumina ratios [20]. Conclusively, the linear increase in the strength of the SCBA-incorporated concrete was due to the pozzolanic activity of SCBA.

3.4. Sorptivity Test

The “index of the moisture transport into unsaturated specimens and it has also been accepted as an important guide for concrete durability” is sorptivity [47–49]. During sorption, water rises into the connected capillary pores as time increases when concrete is exposed to moisture. Therefore, concrete is susceptible to the capillary rise of water through permeable connected pores when exposed to saturated soil, which is normally mimicked by concrete foundations. The sorptivity values at different ages for all the concrete mixes are graphically depicted in Figure 10. The percentage reduction in sorptivity compared to the control concrete for the SCBA-incorporated concretes was 8.32–45.16%, 13.30–41.48%, 15.32–46.77%, and 9.35–25.89% after 7, 28, 56, and 90 days, respectively. The sorptivity of concrete decreases upon the incorporation of SCBA as well as along curing ages. The experimental data show a significant decrease in sorptivity values with the incorporation of SCBA even at 7 days of curing, which is attributed to the clogging of pores by the filler effect of ground SCBA in concrete. The finer particle size, as well as the amorphous silica in SCBA, enhances its pozzolanic activity in the cementitious matrix, thus, densifying the microstructure by greater calcium silicate hydrate gel formation [50].

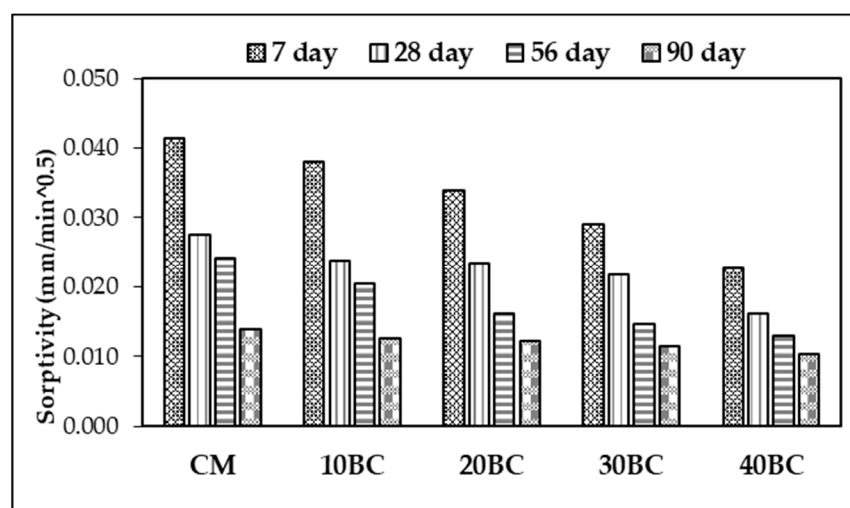


Figure 10. Sorptivity values at different replacement levels of SBA.

The published literature has reported the reduction in sorptivity upon the incorporation of pozzolan-based ashes in concrete. Amin [51] reported that the ground SCBA particles cause the clogging of pores in concrete by the filler effect, thus reducing the penetration of water. However, the maximum reduction of 46.77% in sorptivity compared to the control concrete was recorded at 56 days of curing, demonstrating the maximum

level of pozzolanic activity which corresponds to the clogging of interconnected capillary pores by the generation of pozzolanic hydrates. Similarly, Rajasekar et al. [52] also reported the maximum decrease in SCBA-incorporated concrete's sorptivity at 56 days of curing, in which the maximum decrease in sorptivity was recorded as 42% from the control concrete.

The ratios of cumulative absorption to the square root of time of the corresponding concrete mixes are shown in Figure 11. The trends of sorptivity can be interpolated from polynomial regression equations which are plotted in Figure 11. All the trend lines have a negative slope, indicating the decreasing trends of sorptivity along with increasing SCBA content at varying curing ages. The correlation coefficients were found to be ≥ 0.92 .

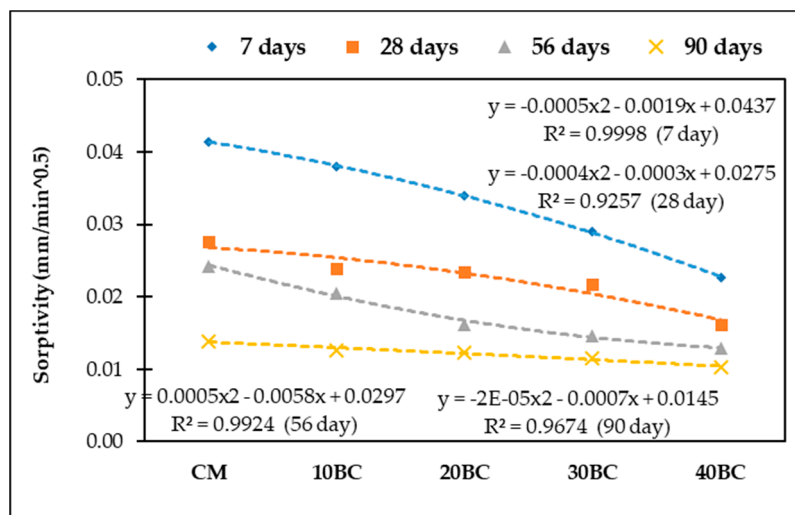


Figure 11. Regression equations for sorptivity.

3.5. Ultrasonic Pulse Velocity (UPV)

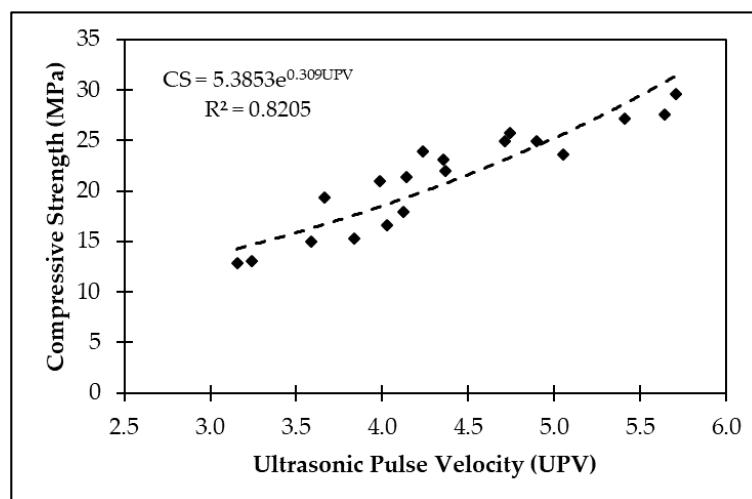
Concrete quality based on its unit weight and the uniformity of the compactness of concrete microstructure can be assessed by ultrasonic pulse velocity [51]. The UPV values of the control and bagasse ash concrete mixtures are shown in Table 5. The increase in UPV values for the CM, 10BC, 20BC, 30BC, and 40BC between 7 and 28 days was 13.35, 16.43, 15.00, 15.31, and 15.20%; between 28 and 56 days it was 13.22, 17.22, 14.49, 9.52, and 2.28%; and between 56 and 90 days it was recorded as 14.86, 20.62, 18.98, 24.71, and 19.60%, respectively. The quality of concrete containing various percentages of SCBA on and above 28 days of curing is graded as good quality concrete as per BIS 13311-92-Part-I as shown in Table 5. Based on this classification, the CM, 10BC, 20BC, and 30BC, 40BC concrete mixes can be classified as of excellent and good quality at 28 days of curing, respectively. Moreover, the 10BC and 20BC mixes had achieved good quality at 7 days of curing similar to that of the control concrete. The increase in UPV value of the 10BC mix compared to the CM was 0.5% at 28 days, which significantly increased to 3.8 and 8.4% at 56 and 90 days of curing. The UPV values increased with the increasing curing age due to the higher percentage of strength development attributed to cement hydration. The prominent increase in UPV values at higher curing ages was due to the dense microstructure of the concrete mixes containing SCBA attributed to the formation of pozzolanic hydrates. Hence, it can be concluded that, despite the lower strength development rate at 7 days of the concrete mixes containing 10% SCBA, the mentioned mixes ultimately gained higher strength development than the control concrete at 28 days and onward.

Table 5. Ultrasonic pulse velocity and concrete quality grading as per BIS 13311-92-Part-I.

Mix	Ultrasonic Pulse Velocity(m/s)				Concrete Quality Grading as per BIS 13311-92-Part-I	
	7 d	28 d	56 d	90 d	Pulse Velocity(m/s)	Concrete quality grading
CM	3670	4160	4710	5410	Above 4500	Excellent
10BC	3590	4180	4900	5910	3500–4500	Good
20BC	3600	4140	4740	5640	3000–3500	Medium
30BC	3460	3990	4370	5450	Less than 3000	Doubtful
40BC	3420	3940	4030	4820		

Published research findings have assessed the SCBA-incorporated concrete on UPV based on the densification of concrete microstructure on its strength development rate. Arenas-Piedrahita et al. [52] utilized untreated SCBA in cement mortar as SCM and reported that its 10% incorporation resulted in no increase in UPV values compared to the control concrete until 180 days of curing. Another research study [53] reported that the thermal treatment of raw SCBA at 250 °C for 12 h, followed by sieving through a 75 µm sieve, produced better UPV values along with curing ages. However, the UPV values remained lower than that of the control concrete until 56 days. Therefore, the current study reported that the reactivity of SCBA enhanced and produced better results at 28 days of curing by grinding the SCBA after sieving through a 75 µm sieve.

As shown in Figure 12, the correlation between compressive strength and UPV depicts that the UPV values are directly proportionate with the compressive strength. The data points and regression trendline depict a good relationship with the regression coefficient value (R) of 0.82, which can be used for interpolating compressive strength with considerable accuracy.

**Figure 12.** Regression equations for compressive strength corresponding to UPV.

3.6. Thermo-Gravimetric Analysis (TGA)

In order to assess the formation of pozzolanic hydrates in the control and optimum mix (10BC), thermogravimetric analysis was performed. The optimum SCBA incorporation amount of 10% was determined from the 28-day strength results. The percentage weight loss of the mentioned specimens until 900 °C are shown in Figure 13, along with the weight loss values shown in Table 6. The thermogravimetric analysis includes the three temperature ranges associated with the weight loss regions of concrete as per the literature [50]. The first temperature zone between the temperature range of 110 and 300 °C corresponds to the physically absorbed water in hydrates such as C-S-H gel and ettringite. The second

temperature zone between the temperature range of 400 and 600 °C is associated with the dihydroxylation of portlandite, whereas decarbonation of calcium carbonate occurred at the third temperature zone between the temperature range of 750 and 900 °C.

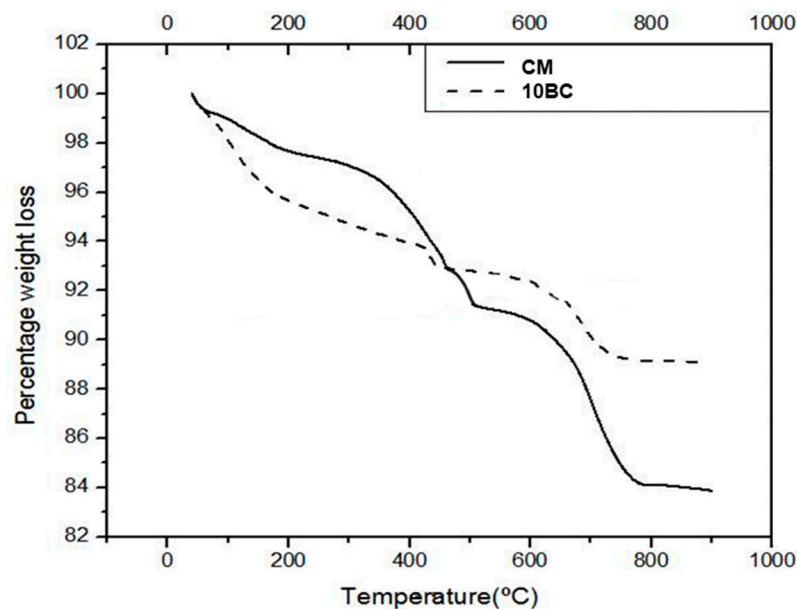


Figure 13. TGA results of control and bagasse mix.

Table 6. Thermogravimetric weight loss of cement paste containing SCBA at 90 days of curing.

Concrete Specimens	Weight Loss (%)			Weight Loss with Respect to Total Weight Loss (%)		
	Stage 1	Stage 2	Stage 3	Stage 1	Stage 2	Stage 3
CM	1.56	1.11	3.72	9.73	6.92	23.22
10BC	1.97	0.84	3.10	16.41	5.79	21.33

The weight loss in the first region of the 10BC mix (1.97%) was higher than that of the control concrete (1.76%), depicting the higher concentration of hydrates in the control concrete. The weight loss of the 10BC mix (0.84%) in the second temperature zone was found to be lower than that of the control concrete (1.11%), marked by lower concentration of portlandite in the 10BC mix that is attributed to the formation of pozzolanic hydrates with the consumption of portlandite in the mentioned mix. Similar results were reported in the literature [54,55] in which a lower concentration of portlandite corresponded to higher pozzolanic activity. The lower percentage of weight loss in the third temperature zone of the 10BC mix is associated with the higher degree of hydration in terms of cumulative concentration of C-S-H and portlandite, which might be due to the nucleation effect of SCBA particles. Hence, the incorporation of processed SCBA produced the pozzolanic hydrates that contributed toward the higher compressive strength (after 28-day age) and densified microstructure compared to the control concrete.

3.7. Acid Attack

Concrete is susceptible to deterioration when exposed to acidic media such as industrial waste waters. Acidic media containing hydrochloric acid and sulfuric acid penetrate into pores and micro-cracks within concrete to cause porosity by accelerated leaching of portlandite and cracking by expansion due to the formation of delayed ettringite formations [1]. The weight loss and strength loss of concrete containing SCBA is shown in Figures 14 and 15, respectively. The effect of sulfuric acid on all concrete specimens was more pronounced than that of hydrochloric acid. It was marked by extensive scaling due

to the reaction of free lime and sulfates which can be visually seen in Figures 16 and 17. The concrete surface immersed in hydrochloric acid showed a rusty brown appearance on the exposed surface that might be due to the formation of ferric chloride by the reaction of iron in cement and chloride in hydrochloric acid. The control concrete exhibited the highest percentage of weight loss and strength loss (9.4% and 47.06%, respectively). However, the percentage of weight loss and strength loss decreased with the incorporation of SCBA in concrete. Thus, the minimum weight and strength losses were recorded for the 40BC mix immersed in hydrochloric acid solution with the values of 3.13% and 13.59%, respectively. The poor performance of the control concrete in acid solution is due to the higher portlandite content in it, which contrarily got consumed in the SCBA-incorporated mixes due to secondary hydrates formation as evidenced by thermogravimetric analysis and the Chapelle test. It is well-known that during the pozzolanic reaction, lower-density portlandite formed during cement hydration is consumed to form the higher-density secondary calcium silicate hydrate gel, thus densifying the concrete microstructure. The densification of the concrete microstructure enhances the resistance to acid penetration into pores and reduces the degree of deterioration caused by acidic media. Arif et al. [56] investigated SCBA use as SCM in cement mortar and found that SCBA incorporation reduced the weight loss and strength loss of mortar upon acid exposure, which might be due to pore refinement.

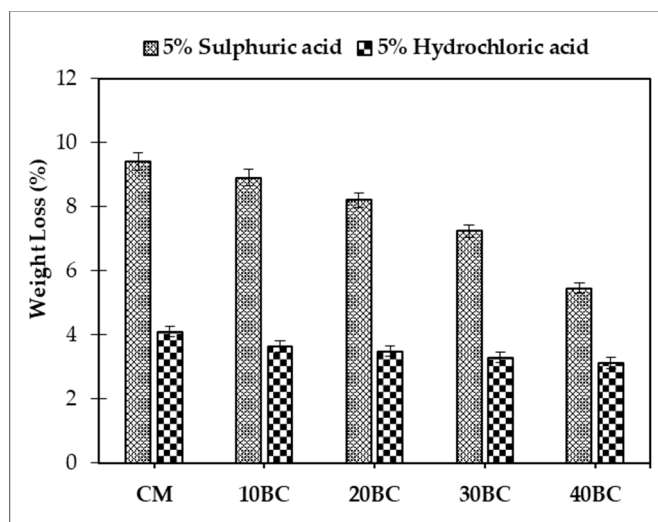


Figure 14. Weight loss of concrete mixes subjected to acid attack.

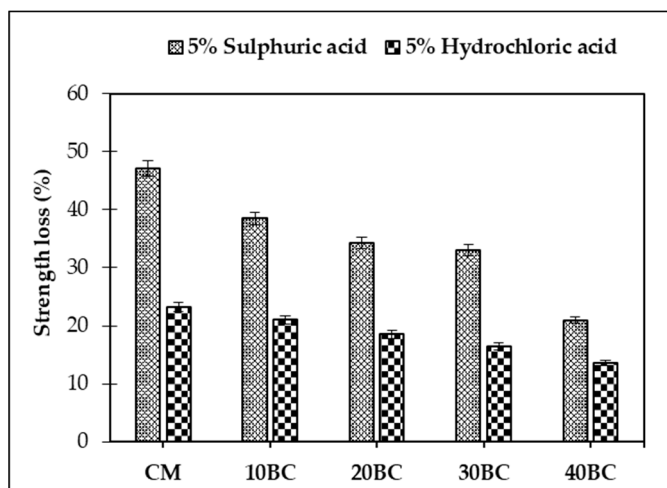


Figure 15. Strength loss of concrete mixes subjected to acid attack.

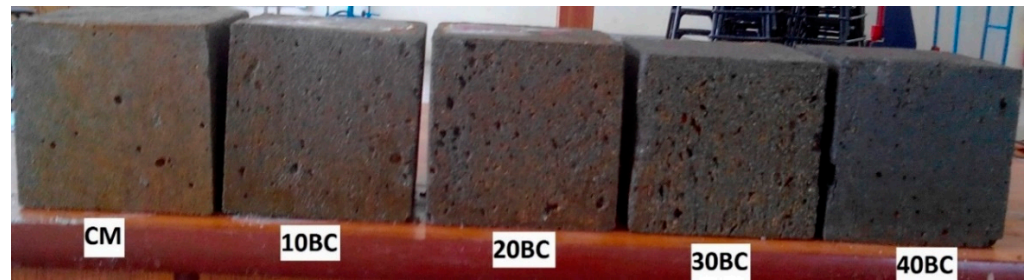


Figure 16. Specimens after immersion in hydrochloric acid.

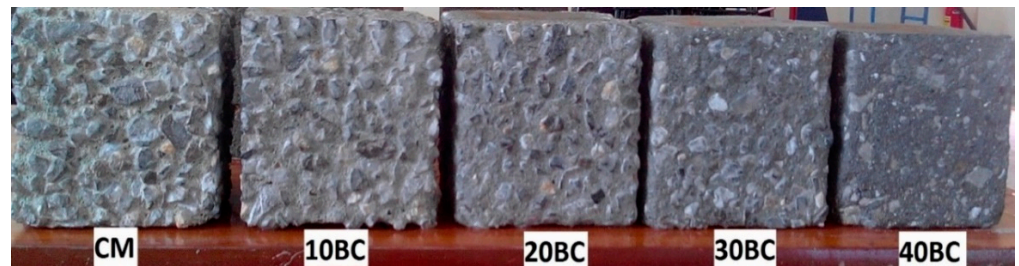


Figure 17. Specimens after immersion in sulfuric acid.

4. Conclusions and Recommendations

The incorporation of processed SCBA as a supplementary cementing material has been corroborated in this research. The following conclusions have been drawn from the analysis of obtained results.

- (a) Most of the SCBA properties comply with that of pozzolan specified in ASTM standard specifications C618-19. SCBA exhibited pozzolanic reactivity as indicated by thermogravimetric analyses and microstructural investigations.
- (b) Fresh concrete properties improved with the SCBA addition which was probably due to the removal of fibrous and unburnt particles. However, the fresh concrete density decreased along with replacing SCBA content, attributed to its lower specific weight.
- (c) The mechanical strength increased with SCBA incorporation and with the increasing testing age. The increase in compressive strength appears to be due to the reactivity of SCBA. At 28 days, the maximum compressive strength with 30% substitution of cement by SCBA resulted in 21 MPa; hence, it can be used for structural applications when used up to 30% replacement of cement.
- (d) The water absorption and sorptivity of concrete decreased with increasing SCBA incorporation due to the filler effect and clogging of pores by the formation of pozzolanic hydrates.
- (e) The quality of most of the concrete mixes containing SCBA has been classified as excellent based on UPV values as per BIS:13311-92 which corresponds to the densified microstructure.
- (f) SCBA-incorporated concrete offered better resistance to sulfuric acid and hydrochloric acid than that of the control concrete. However, the sulfuric acid had more pronounced deterioration in terms of scaling than the damage caused by the hydrochloric acid, which was due to delayed ettringite formation in the case of the former.
- (g) Thermogravimetric analysis results depicted the extent of higher pozzolanic reaction upon the incorporation of SCBA by consumption of portlandite in the cement paste matrix.

In conclusion, the successful utilization of treated SCBA as supplementary cementitious material shall enhance its pozzolanic reactivity in concrete and may reduce the waste disposal carbon emission due to cement production. For future research, the durability per-

formance, including frost resistance and resistance to cyclic loading, must be investigated in detail.

Author Contributions: Conceptualization, S.A.M.; data curation, M.I.S.; formal analysis, S.A.M., U.J., and A.H.; methodology, S.A.M.; investigation, M.I.S.; writing—original draft, S.A.M. and U.J.; supervision, S.A.M.; visualization, U.J.; writing—review and editing, S.A.M., U.J., and A.H.; funding acquisition, S.A.M. All authors have read and agreed to the published version of the manuscript.

Funding: The article processing charges will be funded by Nazarbayev University faculty-development competitive research grants (021220FD0651).

Data Availability Statement: The data used to support the findings of this study are included within the article.

Acknowledgments: The authors acknowledge the support provided by the lab staff in the concrete lab at COMSATS University Islamabad (Abbottabad Campus).

Conflicts of Interest: The authors declare no conflict of interest.

References

1. Li, Z. *Advanced Concrete Technology*; John Wiley & Sons, Inc.: Hoboken, NJ, USA, 2011.
2. Lee, H.; Hanif, A.; Usman, M.; Sim, J.; Oh, H. Performance evaluation of concrete incorporating glass powder and glass sludge wastes as supplementary cementing material. *J. Clean. Prod.* **2018**, *170*, 683–693. [[CrossRef](#)]
3. Olivier, J.G.J.; Peters, J.A.H.W.; Janssens-Maenhout, G. *Trends in Global CO₂ Emissions. 2012 Report*; EU Publications: The Hague, The Netherlands, 2012. [[CrossRef](#)]
4. Yang, H.J.; Usman, M.; Hanif, A. Suitability of Liquid Crystal Display (LCD) Glass Waste as Supplementary Cementing Material (SCM): Assessment based on strength, porosity, and durability. *J. Build. Eng.* **2021**, *42*, 102793. [[CrossRef](#)]
5. Huntzinger, D.N.; Eatmon, T.D. A life-cycle assessment of Portland cement manufacturing: Comparing the traditional process with alternative technologies. *J. Clean. Prod.* **2009**, *17*, 668–675. [[CrossRef](#)]
6. Hanif, A.; Diao, S.; Lu, Z.; Fan, T.; Li, Z. Green lightweight cementitious composite incorporating aerogels and fly ash cenospheres—Mechanical and thermal insulating properties. *Constr. Build. Mater.* **2016**, *116*, 422–430. [[CrossRef](#)]
7. Kim, Y.; Hanif, A.; Usman, M.; Munir, M.J.; Kazmi, S.M.S.; Kim, S. Slag waste incorporation in high early strength concrete as cement replacement: Environmental impact and influence on hydration; durability attributes. *J. Clean. Prod.* **2018**, *172*, 3056–3065. [[CrossRef](#)]
8. Chen, J.; Li, C.; Ristovski, Z.; Milic, A.; Gu, Y.; Islam, M.S.; Wang, S.; Hao, J.; Zhang, H.; He, C.; et al. A review of biomass burning: Emissions and impacts on air quality, health and climate in China. *Sci. Total Environ.* **2017**, *579*, 1000–1034. [[CrossRef](#)]
9. Samad, S.; Shah, A. Role of binary cement including Supplementary Cementitious Material (SCM), in production of environmentally sustainable concrete: A critical review. *Int. J. Sustain. Built Environ.* **2017**, *6*, 663–674. [[CrossRef](#)]
10. Modani, P.O.; Vyawahare, M. Utilization of bagasse ash as a partial replacement of fine aggregate in concrete. *Procedia Eng.* **2013**, *51*, 25–29. [[CrossRef](#)]
11. Kawashima, A.B.; de Moraes, M.V.B.; Martins, L.D.; Urbina, V.; Rafee, S.A.A.; Capucim, M.N.; Martins, J.A. Estimates and Spatial Distribution of Emissions from Sugar Cane Bagasse Fired Thermal Power Plants in Brazil. *J. Geosci. Environ. Prot.* **2015**, *3*, 72–76. [[CrossRef](#)]
12. Gao, S.; Hegg, D.A.; Hobbs, P.V.; Kirchstetter, T.W.; Magi, B.; Sadilek, M. Water-soluble organic components in aerosols associated with savanna fires in southern Africa: Identification, evolution, and distribution. *J. Geophys. Res. D Atmos.* **2003**, *108*. [[CrossRef](#)]
13. Zhang, H.; Wang, S.; Hao, J.; Wang, X.; Wang, S.; Chai, F.; Li, M. Air pollution and control action in Beijing. *J. Clean. Prod.* **2016**, *112*, 1519–1527. [[CrossRef](#)]
14. Lee, B.-J.; Kim, B.; Lee, K. Air pollution exposure and cardiovascular disease. *Toxicol. Res.* **2014**, *30*, 71–75. [[CrossRef](#)] [[PubMed](#)]
15. Sultana, M.S.; Rahman, M.A.; Zaman, M.N.; Ahmed, A.N. Influence of Calcination on Different Properties of Sugarcane Bagasse and Waste Ash. *J. Sci. Res.* **2015**, *7*, 151–157. [[CrossRef](#)]
16. Cordeiro, G.C.; Toledo Filho, R.D.; Tavares, L.M.; Fairbairn, E.D. Ultrafine grinding of sugar cane bagasse ash for application as pozzolanic admixture in concrete. *Cem. Concr. Res.* **2009**, *39*, 110–115. [[CrossRef](#)]
17. Cordeiro, G.C.; Barroso, T.R.; Filho, R.T. Enhancement of the Properties of Sugar Cane Bagasse Ash with High Carbon Content by a Controlled Re-calcination Process. *KSCE J. Civ. Eng.* **2018**, *22*, 1250–1257. [[CrossRef](#)]
18. Rukzon, S.; Chindaprasit, P. Utilization of bagasse ash in high-strength concrete. *Mater. Des.* **2012**, *34*, 45–50. [[CrossRef](#)]
19. Sebastin, S.; Priya, A.K.; Karthick, A.; Sathyamurthy, R.; Ghosh, A. Agro Waste Sugarcane Bagasse as a Cementitious Material for Reactive Powder Concrete. *Clean Technol.* **2020**, *2*, 476–491. [[CrossRef](#)]
20. Xu, Q.; Ji, T.; Gao, S.-J.; Yang, Z.; Wu, N. Characteristics and applications of sugar cane bagasse ash waste in cementitious materials. *Materials* **2018**, *12*, 39. [[CrossRef](#)]
21. Bahurudeen, A.; Kanraj, D.; Dev, V.G.; Santhanam, M. Performance evaluation of sugarcane bagasse ash blended cement in concrete. *Cem. Concr. Compos.* **2015**, *59*, 77–88. [[CrossRef](#)]

22. ASTM C204-18e1; Standard Test Methods for Fineness of Hydraulic Cement by Air-Permeability Apparatus. ASTM International: West Conshohocken, PA, USA, 2019.
23. ASTM C618-19; Standard Specification for Coal Fly Ash and Raw or Calcined Natural Pozzolan for Use in Concrete. ASTM International: West Conshohocken, PA, USA, 2019. Available online: www.astm.org (accessed on 2 October 2022). [[CrossRef](#)]
24. Morales, E.; Villar-Cociña, E.; Frías, M.; Santos, S.; Savastano, H. Effects of calcining conditions on the microstructure of sugar cane waste ashes (SCWA): Influence in the pozzolanic activation. *Cem. Concr. Compos.* **2009**, *31*, 22–28. [[CrossRef](#)]
25. Sultana, M.S.; Rahman, A. Characterization of calcined sugarcane bagasse sugarcane waste ash for industrial use. In Proceedings of the International Conference on Mechanical, Industrial and Materials Engineering 2013 (ICMIME2013), Rajshahi, Bangladesh, 1–3 November 2013; pp. 508–513.
26. E Stutzman, P.; Centeno, L. Compositional Analysis of Beneficiated Fly Ashes. In *Building & Fire Research Laboratory*; National Institute of Standards and Technology: Gaithersburg, MD USA, 1995; p. 19.
27. Quarcioni, V.A.; Chotoli, F.F.; Coelho, A.C.V.; Cincotto, M.A. Indirect and direct Chapelle’s methods for the determination of lime consumption in pozzolanic materials Métodos de ensaio indiretos e método Chapelle direto para determinação do consumo de cal pelos materiais pozolânicos. *Rev. Ibracon Estrut. Mater.* **2015**, *8*, 1–7. [[CrossRef](#)]
28. Pontes, J.; Silva, A.S.; Faria, P. Evaluation of pozzolanic reactivity of artificial pozzolans. *Mater. Sci. Forum.* **2013**, *730*, 433–438. [[CrossRef](#)]
29. Snellings, R.; Kazemi-Kamyab, H.; Nielsen, P.; Van Den Abeele, L. Classification and Milling Increase Fly Ash Pozzolanic Reactivity. *Front. Built Environ.* **2021**, *7*, 1358–1370. [[CrossRef](#)]
30. Bahurudeen, A.; Santhanam, M. Influence of different processing methods on the pozzolanic performance of sugarcane bagasse ash. *Cem. Concr. Compos.* **2015**, *56*, 32–45. [[CrossRef](#)]
31. ASTM C511-03; Standard Specification for Mixing Rooms, Moist Cabinets, Moist Rooms, and Water Storage Tanks Used in the Testing of Hydraulic Cements and Concretes. ASTM International: West Conshohocken, PA, USA, 2003. [[CrossRef](#)]
32. ASTM C143-C143M-12; Standard Test Method for Slump of Hydraulic-Cement Concrete. ASTM International: West Conshohocken, PA, USA, 2015.
33. ASTM C138/C138M-13-01a; Standard Test Method for Density (Unit Weight), Yield, and Air Content (Gravimetric). ASTM International: West Conshohocken, PA, USA, 2001. [[CrossRef](#)]
34. BS 1881-103; Testing Concrete Part 103: Method for Determination of Compacting Factor. British Standards Institution: London, UK, 1993.
35. ASTM C642-13; Standard Test Method for Density, Absorption, and Voids in Hardened Concrete | Engineering360. ASTM International: West Conshohocken, PA, USA, 2013.
36. ASTM C597-16; Standard Test Method for Pulse Velocity Through Concrete. ASTM International: West Conshohocken, PA, USA, 2016.
37. Ballim, Y. Curing and the durability of OPC, fly ash and blast-furnace slag concretes. *Mater. Struct.* **1993**, *26*, 238–244. [[CrossRef](#)]
38. Scrivener, K.; Snellings, R.; Lothenbach, B. *A Practical Guide to Microstructural Analysis of Cementitious Materials*; CRC Press: Boca Raton, FL, USA, 2018. [[CrossRef](#)]
39. Chusilp, N.; Jaturapitakkul, C.; Kiattikomol, K. Utilization of bagasse ash as a pozzolanic material in concrete. *Constr. Build. Mater.* **2009**, *23*, 3352–3358. [[CrossRef](#)]
40. Shafiq, N.; Hussein, A.A.E.; Nuruddin, M.F.; Al Mattarneh, H. Effects of sugarcane bagasse ash on the properties of concrete. *Proc. Inst. Civ. Eng. Sustain.* **2018**, *171*, 123–132. [[CrossRef](#)]
41. Zareei, S.A.; Ameri, F.; Bahrami, N. Microstructure, strength, and durability of eco-friendly concretes containing sugarcane bagasse ash. *Constr. Build. Mater.* **2018**, *184*, 258–268. [[CrossRef](#)]
42. Le, D.-H.; Sheen, Y.-N.; Lam, M.N.-T. Fresh and hardened properties of self-compacting concrete with sugarcane bagasse ash–slag blended cement. *Constr. Build. Mater.* **2018**, *185*, 138–147. [[CrossRef](#)]
43. Jeong, D.-G.; Lee, H.-S. The effect of Pozzolanic reaction under different curing temperatures in strength development of RPC. In Proceedings of the SB10 Seoul International Conference on Sustainable Building Asia, Seoul, Korea, 24–26 February 2010.
44. Mehta, P.K.; Monteiro, P.J.M. *Concrete: Microstructure, Properties and Materials*, 3rd ed.; McGraw-Hill Companies: New York, NY, USA, 2006.
45. Amin, N. Use of Bagasse Ash in Concrete and Its Impact on the Strength and Chloride Resistivity. *J. Mater. Civ. Eng.* **2011**, *23*, 717–720. [[CrossRef](#)]
46. Rajasekar, A.; Arunachalam, K.; Kottaisamy, M.; Saraswathy, V. Durability characteristics of Ultra High Strength Concrete with treated sugarcane bagasse ash. *Constr. Build. Mater.* **2018**, *171*, 350–356. [[CrossRef](#)]
47. Singh, M.; Siddique, R. Properties of concrete containing high volumes of coal bottom ash as fine aggregate. *J. Clean. Prod.* **2015**, *91*, 269–278. [[CrossRef](#)]
48. Dias, W. Reduction of concrete sorptivity with age through carbonation. *Cem. Concr. Res.* **2000**, *30*, 1255–1261. [[CrossRef](#)]
49. Booya, E.; Gorospe, K.; Ghaednia, H.; Das, S. Durability properties of engineered pulp fibre reinforced concretes made with and without supplementary cementitious materials. *Compos. Part B Eng.* **2019**, *172*, 376–386. [[CrossRef](#)]
50. Scrivener, K.L.; Juilland, P.; Monteiro, P.J. Advances in understanding hydration of Portland cement. *Cem. Concr. Res.* **2015**, *78*, 38–56. [[CrossRef](#)]

51. Arshad, M.; Ahmad, S.; Khitab, A.; Hanif, A. Synergistic Use of Fly Ash and Silica Fume to Produce High-Strength Self-Compacting Cementitious Composites. *Crystals* **2021**, *11*, 915. [[CrossRef](#)]
52. Arenas-Piedrahita, J.; Montes-García, P.; Mendoza-Rangel, J.; Calvo, H.L.; Valdez-Tamez, P.; Martínez-Reyes, J. Mechanical and durability properties of mortars prepared with untreated sugarcane bagasse ash and untreated fly ash. *Constr. Build. Mater.* **2016**, *105*, 69–81. [[CrossRef](#)]
53. Quedou, P.G.; Wirquin, E.; Bokhoree, C. Sustainable concrete: Potency of sugarcane bagasse ash as a cementitious material in the construction industry. *Case Stud. Constr. Mater.* **2021**, *14*, e00545. [[CrossRef](#)]
54. Memon, S.A.; Javed, U.; Khushnood, R.A. Eco-friendly utilization of corncob ash as partial replacement of sand in concrete. *Constr. Build. Mater.* **2019**, *195*, 165–177. [[CrossRef](#)]
55. Javed, U.; Khushnood, R.A.; Memon, S.A.; Jalal, F.E.; Zafar, M.S. Sustainable incorporation of lime-bentonite clay composite for production of ecofriendly bricks. *J. Clean. Prod.* **2020**, *263*, 121469. [[CrossRef](#)]
56. Arif, E.; Clark, M.W.; Lake, N. Sugar cane bagasse ash from a high efficiency co-generation boiler: Applications in cement and mortar production. *Constr. Build. Mater.* **2016**, *128*, 287–297. [[CrossRef](#)]